Radiative recombination between fully stripped ions and free electrons

Lars H. Andersen and Jakob Bolko
Institute of Physics, University of Aarhus, DK-8000 Aarhus C, Denmark
(Received 2 April 1990)

In the present paper we report on measurements of the rate coefficient for radiative recombination between free electrons and bare ions. The measurements were done with merging beams of electrons and 2-MeV/amu fully stripped He, C, and F ions. Relative energies between 0 and 1 eV were considered. In the low-energy limit, calculations of the n and l distribution of the cross section, according to the "exact" theory by Stobbe, are presented for values of n up to 60. It is shown that corrections to the Bethe and Salpeter theory are needed for capture to the low-n states. The experimental data are compared with a calculation based on the Bethe and Salpeter theory as well as a calculation based on Stobbe's theory for $n \leq 3$ and the Bethe and Salpeter theory for $n > 3$.

I. INTRODUCTION

Because of the coupling between matter and the electromagnetic field, it is possible for an electron to make a transition from one state to another under the emission of light. When two bound states are involved, the process results in emission of light with discrete wavelength, the wavelength being characteristic of the two states involved. When two continuum states are involved, the free-free transition, a continuous spectrum of light is emitted, and the process is known as bremstralung. In the present paper, we shall deal with the situation where the initial state of the electron is an unbound state, and the final state is a bound one, the free-bound transition. This is known as radiative recombination (RR) or radiative electron capture. As for bremsstralung, this process may take place at any initial kinetic energy of the free electron.

In the case of a bare ion the radiative recombination process may be written as

$$X^{Z+}+e^{-}\rightarrow X^{(Z-1)+}(n)+h\nu\ , \tag{1}$$

where $h\nu$ is the emitted photon, the energy of which equals the kinetic energy of the initial free electron plus the binding energy of the hydrogenic level n. X is the bare ion with nuclear charge Z. In the present work, we have measured the rate coefficient for the RR process (1) summed over the final states n, as a function of the nuclear charge Z ($Z=2,6,9$) and the initial energy of the free electron (0–1 eV).

Measurements of radiative recombination with nonbare ions (C^{5+}, O^{7+}, F^{8+}, and O^{5+}) were reported recently.[1] The use of bare ions in the present measurement eliminates the effects of electronic screening. Further, dielectronic recombination that normally is associated with much higher cross sections than RR can be disregarded.

In the past, the process of radiative recombination has attracted a great deal of interest. From a theoretical point of view, the process was the object for several papers starting already in the 1920s.[2–6] In 1923 Kramers,[2] at the Niels Bohr Institute in Copenhagen, used semiclassical arguments to derive the cross section for RR. At that time the quantum theory of radiation was not developed to solve the problem of radiative recombination in detail. Instead the idea of Bohr's correspondence principle was used to obtain an approximate solution. Later, several theoretical papers followed.[7–11] The main theme has been to find appropriate approximations to overcome the large numerical calculations involved. The difficulties mainly stem from the treatment of the excited final states of the recombined ion.

Since the initial and final wave functions are known analytically in the case of a pure Coulomb field from a bare ion, the cross section for radiative recombination may in principle be calculated exactly. In the dipole approximation, the cross section for capture into the hydrogenic level (n,l) is simply given by[6]

$$\sigma_{n,l}=\frac{4}{3}\alpha\frac{\omega^3}{c^2 v_e}|\langle\psi_{nl}|\mathbf{r}|\psi_{\mathbf{k}}\rangle|^2\ , \tag{2}$$

where α is the fine-structure constant, c is the speed of light, ω is the frequency of the emitted light, v_e is the electron velocity in the frame of the ion, ψ_{nl} is the hydrogenic final state, and ψ_k is the initial free state of the electron with wave vector $\mathbf{k}$. In the early work of Stobbe[4] the cross sections for capture into the lowest hydrogenic levels were calculated analytically. Later Bethe and Salpeter[6] derived an approximate analytical formula for the cross section for RR. In their work, advantage was taken of the fact that the oscillator strength crosses the continuum limit smoothly. Thus, knowledge about the hydrogenic bound-bound transitions was utilized to derive the cross section for RR. Bethe and Salpeter obtained the following simple expression for the cross section for radiative recombination to a hydrogenic level with main quantum number n:

$$\sigma_n=2.10\times10^{-22}\ \text{cm}^2\frac{Z^4E_0^2}{nE_e(Z^2E_0+n^2E_e)}\ , \tag{3}$$

where E_e is the kinetic energy of the free electron, and E_0

is the Rydberg energy. Due to the approximate way Bethe and Salpeter derived formula (3), corrections must be applied for the lower states. For these states, where the largest cross sections are found, the more accurate calculations by Stobbe yield corrections, which are about 20% for $n=1$, 12% for $n=2$, and 9% for $n=3$, the cross sections of Stobbe being smaller than those of Bethe and Salpeter. Here we have extended the work given by Stobbe and report on the n and l distribution of the cross section for values of n up to 60 in the limit of low kinetic energy of the free electron.

The different electron-ion recombination processes are of considerable interest in connection with laboratory and astrophysical plasmas. Lately, new attention has been paid to the RR process, as the process has been suggested as a method to produce antimatter.[12,13] The radiative recombination between a positron and an antiproton will produce antihydrogen. In order to increase the rate of antihydrogen production it has been proposed to stimulate the recombination process by a laser.[14]

The RR process has been treated theoretically for many years, yet the first direct measurement of the process was not done until very recently, where we succeeded in measuring the rate coefficient for radiative recombination for bare carbon ions.[15] Early attempts to measure the rate coefficient have failed either because the electron gas was too dense,[16] in which case three-body-recombination[17] becomes dominating, or because the energy distribution of the electron gas was not well characterized.[18]

The remaining part of this paper is arranged as follows. First we describe the experiment, then we discuss the theory and present our calculation of the (n,l) cross sections for RR, and finally we compare the measured rate coefficients with theory.

II. EXPERIMENTAL TECHNIQUE

The present experiment was performed at the 6-MV EN tandem accelerator at the University of Aarhus. Beams of He^{2+}, C^{6+}, and F^{9+} were used at an energy of 2 MeV/amu. The experiment is shown in Fig. 1. In order to clean the beam from unwanted charge components created via electron capture in the restgas, the beam was bent 15° immediately in front of the interaction region. The ion current was typically 1 μA. After the interaction region the ions were charge-state-analyzed by an electric field perpendicular to the beam direction. This field sets an upper limit, n_{max}, of the main quantum number for the states on the recombined ions that reaches the position-sensitive channel-plate detector at the end of the beamline. n_{max} was calculated according to[19] the following:

$$n_{max}=(6.2\times10^{8}Z^{3}/E)^{1/4}\ , \tag{4}$$

where E is the electric field in V/cm. Fields on the order of 10–12 kV/cm were applied. The direct beam was collected in a negatively biased Faraday cup.

In order to avoid a large background signal of ions with charge $Z-1$ at the ion detector, the vacuum was kept as low as possible in the beamline. During the measurement, the pressure was in the order of $(1–2)\times10^{-11}$ torr.

From the electron gun, the electrons were accelerated to an energy of about 1100 eV. They then travel with about the same velocity as the ions and thus very small relative energies were obtained. The electron current was typically 10 mA, and the electron beam diameter was 1 cm. As shown in a previous paper,[20] the intensity of the electron beam was almost constant over the size of the electron beam. In order to compensate for the space-charge field, a magnetic field of about 200 G guided the electrons from the gun to the collector. In the region of the ion beam, the mean space-charge potential created by the electrons was about 2 V/cm.

To ensure full overlap between the two beams, electrostatic pickup plates were mounted in the interaction region, by which the position of the beams could be monitored. The ion beam was approximately Gaussian with a width of about 2 mm (2σ), and hence the ion beam was fully confined in the electron beam. This made it possible to determine the rate coefficient on an absolute scale.

To distinguish the signal from the background, we

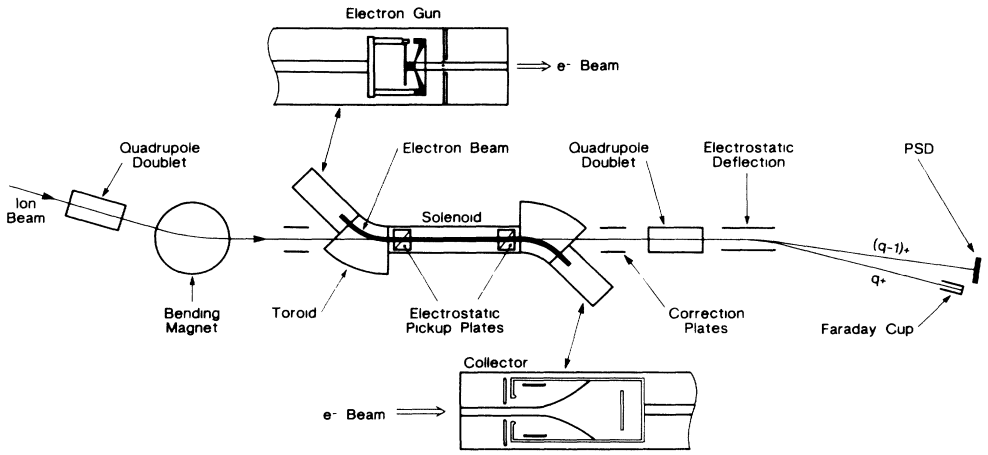

FIG. 1. Experimental setup shown schematically.

used a modulation technique by which the electron beam was chopped at a frequency of 250 Hz. This was done by modulating the anode potential in the electron gun between 0 and -2 kV. Figure 2 demonstrates the principle. When the anode voltage was at -2 kV, the electrons were turned off, since the cathode potential was approximately -1100 V. The rise time of the voltage applied to the anode was 4 μsec. One analog-to-digital converter (ADC) was opened for 1.4 msec in the middle of the 2-msec period, when the electron beam was on, to measure signal plus background. In a similar way, another ADC was opened for 1.4 msec when the electron beam was turned off to measure background signal only. It was verified that the chopping frequency was sufficiently large that the vacuum did not change between the two measuring intervals. Figure 3 shows the yield of charge-changed ions in the two measuring intervals as a function relative energy for 8 MeV He^{2+}. The true RR signal is clearly seen as a symmetric cusp, which peaks a zero relative energy. Negative and positive energies correspond to the situation, where the electrons are slower, respectively faster, than the ions. At each relative energy data were taken for 2 min.

The RR signal was obtained as the difference in yield obtained with and without the electron beam on. The rate coefficient for the RR process was then obtained as

$$\langle v\sigma \rangle = \frac{1}{\varepsilon} \frac{N^{X(Z-1)+} - N_0^{X(Z-1)+}}{N^{X(Z)+}} \frac{v_i}{\rho_e L} , \tag{5}$$

where $N^{X(Z)+}$ is the number of incident ions, $N^{X(Z-1)+}$ is the number of ions with charge $Z-1$ measured with the electron beam on, $N_0^{X(Z-1)+}$ is the corresponding number when the electron beam is off, ρ_e is the electron density, v_i the ion velocity, and ε the ion-detection efficiency, which was directly measured by comparing count rates in a solid-state detector and in the channel-plate detector. L is the length of the section, where the two beams merge. The physical distance between the two totoids was 100 cm. It is known, however, that the effective target length is shorter by typically 10–20 % due to imperfections in the guiding magnetic field.[21,22] Here, the target length L is set equal to 85 cm. In our first report[15] on RR for C^{6+}, we did not correct for this effect in the presentation of the experimental data.

The relation between the measured rate coefficient and the cross section for RR is

$$\langle v\sigma \rangle = \int v\sigma f(\bar{v}) d\bar{v}, \quad \sigma = \sum_{n=1}^{n_{\max}} \sigma_n , \tag{6}$$

where $f(\bar{v})$ is the relative velocity distribution. We chose to represent this distribution by a product of two Maxwell distributions,

$$f(\bar{v}) = \frac{m}{2\pi k T_\perp} e^{-mv_\perp^2/2kT_\perp} \left[\frac{m}{2\pi k T_\parallel} \right]^{1/2} e^{-m(v_\parallel - \Delta)^2/2kT_\parallel} , \tag{7}$$

where $v_\perp$ and $v_\parallel$ are the electron-velocity components perpendicular and parallel to the ion-beam directions, respectively, and Δ is the detuning velocity that defines the relative energy ($\frac{1}{2}m\Delta^2 = E_e$). $T_\perp$ and $T_\parallel$ are the two temperatures[23] that characterize the motion of the electrons relative to the moving frame of the electron beam. Any contribution to the energy spread from the ions is expected to be small, yet it is also included in the two temperatures.

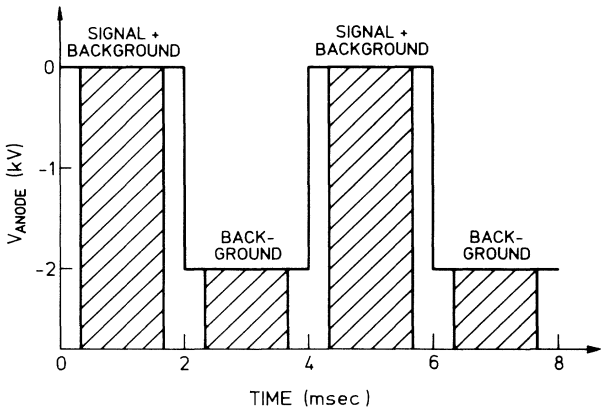

FIG. 2. Anode voltage as a function of time. The dashed areas represent the time when data were taken.

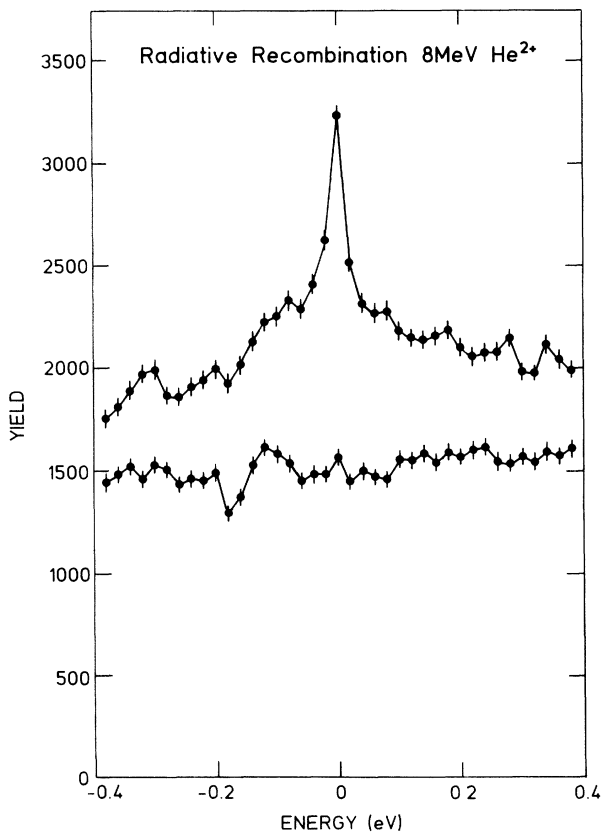

FIG. 3. Yield of He^+ ions as a function of relative energy. The upper data were taken with the electron beam on, and the lower data were taken without the electron beam. The error bars represent the statistical uncertainty. The data shown are not normalized to electron and ion currents.

The electron temperature as defined in Eq. (7) is related to the rest frame and is not identical to the energy resolution of the merged beam experiment.[24] The contribution to the energy spread from the transverse temperature is independent of the relative energy (E_e), whereas the contribution from the longitudinal temperature is proportional to the square root of $kT_{\parallel}E_e$. To be able to compare the rate coefficient obtained from Eq. (5) with theory, one must know $f(\mathbf{v})$, i.e., $T_{\perp}$ and $T_{\parallel}$ must be known.

To determine $T_{\perp}$ and $T_{\parallel}$, we used a 24-MeV C^{4+}-ion beam produced in the same way as the C^{6+} beam. That is, the C^{4+} ions were also created via a post-stripper foil to include angular effects due to scattering in the foil. C^{4+} in the metastable $1s2s$ states exhibits some very sharp dielectronic-recombination resonances,[20,25] the cross section of which may be represented by δ functions. The rate coefficient for the dielectronic-recombination resonance was then calculated according to Eqs. (6) and (7), and $T_{\perp}$ and $T_{\parallel}$ were determined from a fit to the shape of the obtained resonances. In our previous papers,[15,20] we have shown such fits, which yield $kT_{\perp}=0.15$ eV and $kT_{\parallel}=2\times10^{-3}$ eV. As expected, due to the longitudinal acceleration, the velocity distribution is flattened ($kT_{\parallel}\ll kT_{\perp}$).

III. CALCULATION OF THE n,l DISTRIBUTION

Since the Bethe and Salpeter theory yields a simple analytical expression for the cross section for the RR process, we have combined Eqs. (3), (6), and (7) and obtained the following expression for the rate coefficient, measured in cm^3/s, as a function of relative energy E_e:

$$\langle v\sigma\rangle(E_e)=2.30\times10^{-12}\frac{Z^2b\exp(b^2E_e/kT_{\perp})}{kT_{\perp}(kT_{\parallel})^{1/2}}\int_0^{\infty}\sum_{n=1}^{n_{\max}}\frac{\exp(-kT_{\parallel}t^2/kT_{\perp})}{n(n^2t^2/Z^2+E_0/kT_{\parallel})}[\Phi(bx+t/b)-\Phi(bx-t/b)]dt\ , \tag{8}$$

where $b=[T_{\perp}/(T_{\perp}-T_{\parallel})]$ and $x=(E_e/kT_{\parallel})^{1/2}$. All energies are in units of eV. E_0 is the Rydberg energy and Φ is the error function.

As mentioned in the Introduction, the formula (3) as derived by Bethe and Salpeter is only an approximate expression for the RR cross section. We have followed the work of Stobbe and applied Eq. (2) with the relevent wave functions to obtain a more precise result, and in order to extract both the n and l distribution. Equation (2) was derived in the dipole approximation, which is valid for the relative small photon energies considered here. For the final-state wave function, hydrogenic wave functions were used and the continuum wave function was at infinity described by a plane wave. According to Stobbe[4] the cross section for capture to the hydrogenic state n,l is given by

$$\sigma_{nl}=\frac{4\pi}{3}\alpha\frac{\omega^3}{c^2}\frac{1}{k^2}[l|\langle El-1|r|nl\rangle|^2+(l+1)|\langle El+1|r|nl\rangle|^2]\ , \tag{9}$$

where

$$|\langle El|r|n'l-1\rangle|=\frac{(-1)^{n'-l}i}{8k^{3/2}(2l-1)!}\left[\frac{2(n'+l-1)!\prod_{s=1}^{1}[s^2+1/(ak)^2]}{(n'-l)!\sinh(\pi/ak)}\right]^{1/2}e^{[\pi/2-2\arctan(k/k_n)]/ak}\left[\frac{4kk_n}{k_n^2+k^2}\right]^{l+1}u^{n'-l-1}$$
$$\times\left[F\left[l+1-\frac{in'}{ak},l-n',2l,1-u^{-2}\right]-u^2F\left[l-1-\frac{in'}{ak},l-n',2l,1-u^{-2}\right]\right] \tag{10}$$

and

$$|\langle El|r|n'l+1\rangle|=\frac{(-1)^{n'-l-1}a}{8k^{1/2}(2l+1)!}\left[\frac{2(n'+l-1)!\prod_{s=0}^{1}[s^2+1/(ak)^2]}{(n'-l-2)!\sinh(\pi/ak)}\right]^{1/2}$$
$$\times\exp\left[\left[\frac{\pi}{2}-2\arctan\frac{k}{k_n}\right]\Big/ak\right]\left[\frac{4kk_n}{k_n^2+k^2}\right]^{l+2}u^{n'-l-2}$$
$$\times\left[F\left[l+1-\frac{in'}{ak},l+2-n',2l+2,1-u^{-2}\right]-u^2F\left[l+1-\frac{in'}{ak},l-n',2l+2,1-u^{-2}\right]\right]\ , \tag{11}$$

where u and k_n are defined by

$$k_n=(2m|E_e|)^{1/2}/\hbar,\quad u=\frac{k_n+ik}{k_n-ik} \tag{12}$$

and $a=a_0/Z$ is the Bohr radius for an ion with charge $Z+$. F is the well-known hypergeometric function. The expression given in Eqs. (9)–(12) may seem rather simple, yet the cross sections are not easily calculated for the

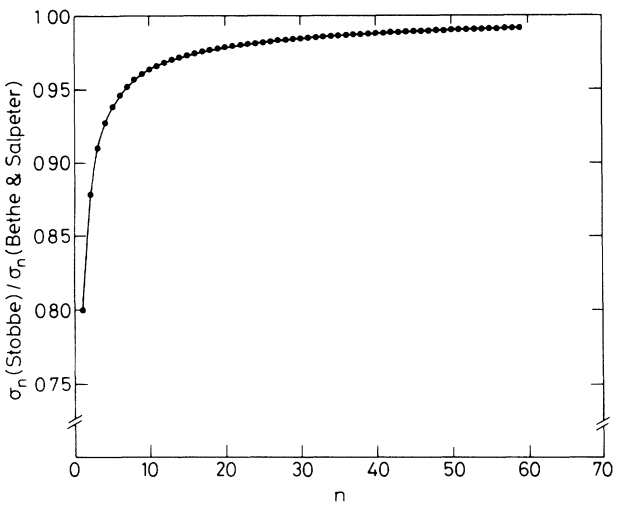

FIG. 4. Cross section σ_n calculated according to Stobbe's theory divided by σ_n calculated from the Bethe and Salpeter formula Eq. (3) as a function of n.

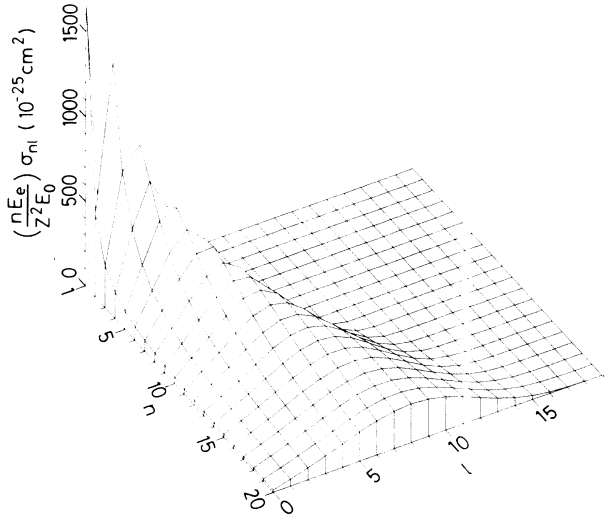

FIG. 5. Scaled cross section $(nE_e/Z^2E_0)\sigma_{nl}$ as a function of n and l.

TABLE I. The reduced RR cross sections $(nE/Z^2E_0)\sigma_{nl}$ in units of 10^{-25} cm^2. The cross sections are calculated according to Stobbe's theory in the limit of small electron energies.

n/l	0	1	2	3	4	5	6	7	8	9	10	11	12	13	14	15	16	17	18	19
1	1678																			
2	491	1351																		
3	248	770	891																	
4	155	491	743	555																
5	108	345	569	611	335															
6	81.5	258	441	546	459	198														
7	64.2	202	351	467	471	325	116													
8	52.3	164	287	396	441	377	221	67.2												
9	43.7	136	239	339	400	385	286	146	38.6											
10	37.2	116	204	292	358	372	317	208	94.3	22.0										
11	32.3	100	176	254	319	349	325	249	147	59.8	12.5									
12	28.3	88.0	154	223	286	324	321	271	189	101	37.3	7.07								
13	25.2	77.9	136	198	256	298	309	281	218	139	68.3	23.0	3.98							
14	22.5	69.7	121	177	231	274	293	281	236	169	99.7	45.2	14.0	2.24						
15	20.4	62.8	109	159	209	252	277	275	245	191	128	70.0	29.5	8.49	1.25					
16	18.5	57.1	99.1	144	191	232	260	267	248	207	151	94.5	48.3	18.9	5.10	0.70				
17	16.9	52.1	90.4	132	174	214	243	256	247	216	169	116	68.3	32.8	12.0	3.04	0.39			
18	15.6	47.9	82.9	121	160	198	228	244	242	221	183	135	87.9	48.5	21.9	7.62	1.80	0.21		
19	14.4	44.2	76.5	111	148	183	213	232	236	222	192	150	105	64.9	33.9	14.5	4.76	1.06	0.12	
20	13.4	41.0	70.8	103	137	170	200	220	228	220	197	162	121	80.9	47.2	23.4	9.50	2.95	0.62	0.06
25	9.73	29.6	50.8	73.6	98.0	123	147	169	185	194	194	183	164	137	108	78.3	52.0	31.2	16.7	7.82
30	7.50	22.7	38.8	56.1	74.5	93.8	113	132	149	162	170	172	167	156	138	117	94.6	71.7	51.0	33.7
35	6.02	18.2	31.0	44.6	59.1	74.4	90.3	106	121	134	145	152	154	152	145	134	119	101	82.7	64.4
40	4.99	15.1	25.6	36.7	48.5	60.9	73.9	87.2	100	112	123	132	138	141	140	135	127	116	102	87.8
45	4.23	12.7	21.6	30.9	40.7	51.1	62.0	73.2	84.5	95.5	105	114	122	127	130	129	126	120	112	101
50	3.65	11.0	18.6	26.5	34.9	43.7	53.0	62.6	72.3	82.1	91.4	100	107	114	118	120	121	118	114	107
55	3.19	9.64	16.2	23.1	30.3	38.0	45.9	54.3	62.8	71.4	79.9	88.0	95.4	101	107	111	113	113	111	108
60	2.83	8.54	14.3	20.4	26.7	33.4	40.4	47.7	55.2	62.8	70.4	77.8	84.9	91.3	96.9	101	104	106	106	105

higher orbitals. Since we are concerned with relative low energies of the free electron (0–1 eV) we have simplified the calculation somewhat by considering the low-energy limit. In this limit the hypergeometric functions F were calculated to the lowest order in k.

In Fig. 4 is shown the calculated cross section σ_n normalized to the result from the Bethe and Salpeter formula [Eq. (3)] as a function of n. It is evident that the simple formula overestimates the cross section for the low n values. This is in agreement with earlier findings.[14] At high values of n, the ratio approaches unity.

In the simplified treatment of Bethe and Salpeter, there is no information on the l distribution. That, however, is contained in the theory by Stobbe. In Fig. 5 and Table I is presented the scaled cross section $(nE_e/Z^2E_0)\sigma_{nl}$ as a function of n and l. Apparently, a range of l values are populated via radiative recombination. At increasing values of n the main contribution to σ_n comes from the lower l states. For $n=60$ we find that the most populated angular momentum state is $l=18$.

IV. RESULTS AND DISCUSSION

The experimental data for He^{2+}, C^{6+}, and F^{9+} are shown in Fig. 6. In order to improve the statistics, the data are averaged over the two sides of the "cusp" shown in Fig. 3. The data are compared to the rate coefficient obtained from the Bethe and Salpeter formula [Eqs. (3) and (8)] and the Bethe and Salpeter theory corrected for $n=1$, 2, and 3 according to Stobbe.[4] The Bethe and Salpeter rate coefficient was multiplied by 0.794 for $n=1$, 0.877 for $n=2$, and 0.909 for $n=3$, independent of the relative energy. Due to the relative low population of the higher n states the small corrections to these states were neglected. In the calculation of the rate coefficient we used 0.15 eV for the transverse temperature and 0.002 eV for the longitudinal temperature as was found previously.[15,20] Values of n smaller than n_{max} were included, where n_{max} was 27, 60, and 78 for He, C, and F ions, respectively. Within the error bars of the experiment there is agreement between both calculations and the experiment. The corrections introduced for $n=1$, 2, and 3 based on the theory by Stobbe results in a lowering of the Bethe and Salpeter theory by about 8%.

The dependence of the rate coefficient on the two electron temperatures is shown in Figs. 7 and 8. Figure 7 shows the rate coefficient for radiative recombination with C^{6+} ions for three different transverse temperatures and a constant longitudinal temperature. At the largest energy (1 eV), the rate coefficient becomes essentially independent of $kT_\perp$ as expected in the limit $kT_\perp \ll E_e$. At lower energies, a pronounced dependence is found. The

TABLE I. (*Continued*).

20	21	22	23	24	25	26	27	28	29	30	31	32	33	34	35	36	37	38	39
3.10	1.00	0.24	0.04	0.00															
20.6	11.5	5.81	2.60	1.01	0.33	0.09	0.01	0.00	0.00										
47.6	33.4	22.0	13.6	7.81	4.13	1.99	0.86	0.33	0.11	0.03	0.00	0.00	0.00	0.00					
72.3	57.3	43.5	31.7	21.9	14.4	8.99	5.25	2.87	1.45	0.68	0.28	0.11	0.03	0.01	0.00	0.00	0.00	0.00	0.00
89.4	76.4	63.4	50.8	39.3	29.3	21.0	14.4	9.51	5.94	3.52	1.97	1.03	0.50	0.23	0.09	0.03	0.01	0.00	0.00
99.0	89.0	78.1	66.8	55.6	45.0	35.3	26.8	19.7	14.0	9.56	6.27	3.93	2.35	1.34	0.72	0.36	0.17	0.07	0.03
102	95.8	87.5	78.3	68.5	58.6	48.9	39.8	31.6	24.4	18.2	13.2	9.32	6.32	4.13	2.60	1.57	0.90	0.49	0.26
102	98.2	92.4	85.4	77.5	69.0	60.2	51.5	43.1	35.3	28.2	22.0	16.7	12.3	8.89	6.20	4.18	2.73	1.72	1.04

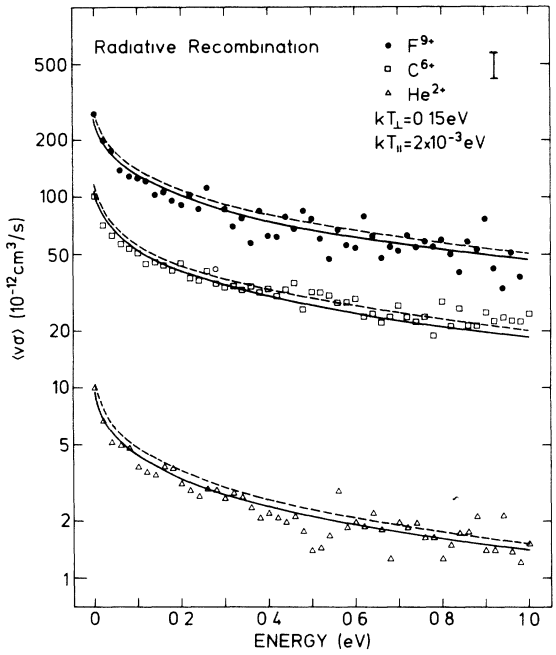

FIG. 6. Experimental rate coefficient $\langle v\sigma \rangle$ as a function of relative energy for He^{2+}, C^{6+}, and F^{9+}. The dashed curve is the rate coefficient obtained with the Bethe and Salpeter cross section, and the full curve is the same calculation corrected for $n=1$, 2, and 3 according to Stobbe. The error bar shows the uncertainty from the determination of the target length, which was put equal to 85±15 cm.

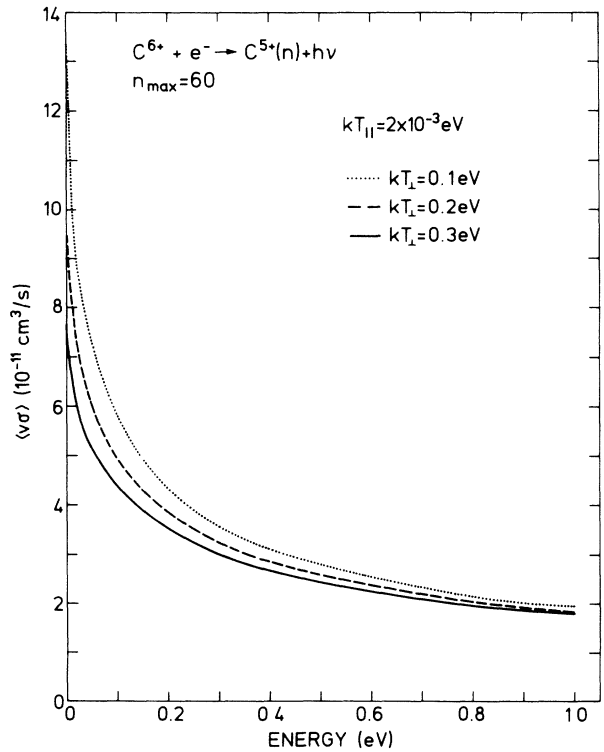

FIG. 7. Rate coefficient for C^{6+} as a function of relative energy. Three curves are shown corresponding to $kT_\perp=0.1$ eV (· · · ·) 0.2 eV (— — —), and 0.3 eV (——). The curves are the theory of Bethe and Salpeter corrected according to Stobbe for $n=1$, 2, and 3.

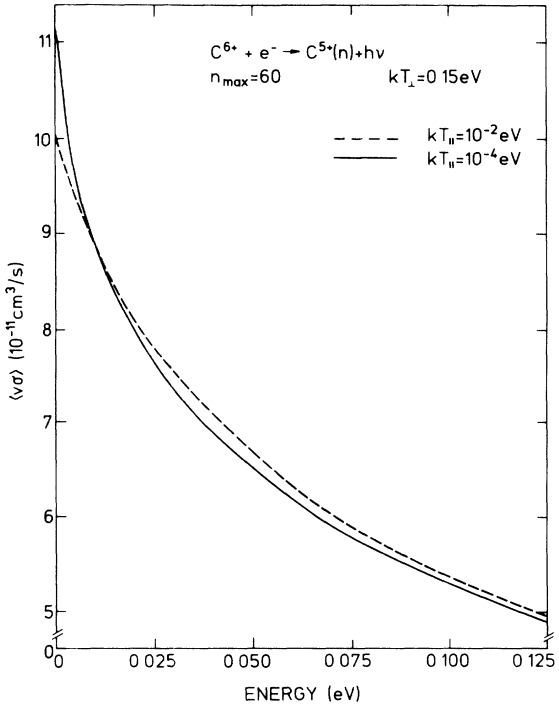

FIG. 8. Rate coefficient for C^{6+} as a function of relative energy. Shown is the dependence of the longitudinal temperature. — — —, $kT_\parallel=10^{-2}$ eV; ——, 10^{-4} eV. — — — 0.2 eV; and —— 0.3 eV. The curves are the theory of Bethe and Salpeter corrected according to Stobbe for $n=1$, 2, and 3.

dependence on $T_\parallel$ is much weaker. A change in the longitudinal temperature from 0.0001 to 0.01 eV only changes the rate coefficient noticeable at very small relative energies as shown in Fig. 8.

V. CONCLUSION

The process of radiative recombination has been measured for bare ions and low-energy electrons. It is found that the rate coefficient $\langle v\sigma \rangle$ for radiative recombination is reasonably well described by the simple Bethe and Salpeter formula. A calculation of the RR cross section based on the theory of Stobbe shows that corrections are needed for the lower n states, whereas for the high n states the cross sections are well predicted by the Bethe and Salpeter formula. The l dependence of the RR cross section was calculated from the Stobbe theory, and it was found that a broad range of l values are populated via RR in the limit of low-impact energy.

ACKNOWLEDGMENTS

This work has been supported by the Danish National Science Research Council, the Carlsberg Foundation, and the Ib Henriksen Foundation.

[1]L. H. Andersen and J. Bolko (unpublished).
[2]H. A. Kramers, Philos. Mag. **46**, 836 (1923).
[3]J. R. Oppenheimer, Phys. Rev. **31**, 349 (1928).
[4]M. Stobbe, Ann. Phys. **7**, 661 (1930).
[5]W. Wessel, Ann. Phys. **5**, 611 (1930).
[6]H. Bethe and E. Salpeter, *Quantum Mechanics of One- and Two-Electron Systems*, Vol. 35 of *Handbuch der Physik* (Springer, Berlin, 1957).
[7]C. M. Lee and R. H. Pratt, Phys. Rev. A **14**, 990 (1976).
[8]Y. Hahn and D. W. Rule, J. Phys. B **10**, 2689 (1977).
[9]V. M. Kathov and V. M. Strakhovenko, Zh. Eksp. Teor. Fiz. **75**, 1269 (1978) [Sov. Phys.—JETP **48**, 639 (1978)].
[10]Y. S. Kim and R. H. Pratt, Phys. Rev. A **27**, 2913 (1983).
[11]A. I. Milstein, Phys. Lett. A **136**, 52 (1989).
[12]G. I. Budker and A. N. Skrinskii, Usp. Fiz. Nauk **124**, 561 (1978) [Sov. Phys.—Usp. **21**, 277 (1978)].
[13]H. Herr, D. Mohl, and A. Winnacker, in *Proceedings of the Workshop on Physics at LEAR with Low-Energy-Cooled Antiprotons, Erice, 1982,* edited by U. Gastaldi and R. Klapisch (Plenum, New York, 1984) p. 659; H. Poth, Phys. Scr. **38**, 806 (1988).
[14]R. Neumann, H. Poth, A. Winnacker, and A. Wolf, Z. Phys. A **313**, 253 (1983).
[15]L. H. Andersen, J. Bolko, and P. Kvistgaard, Phys. Rev. Lett. **64**, 729 (1990).
[16]See, e.g., N. D'Angelo, Phys. Rev. **121**, 505 (1961).
[17]See, e.g., J. Stevefelt, J. Boulmer, and J-F. Delpech, Phys. Rev. A **12**, 1246 (1975).
[18]H. Poth *et al.*, Z. Phys. A **332**, 171 (1989).
[19]F. Brouillard, in *Atomic and Molecular Processes in Controlled Thermonuclear Fusion*, edited by C. J. Jochain and D. E. Post (Plenum, New York, 1983).
[20]L. H. Andersen, J. Bolko, and P. Kvistgaard, Phys. Rev. A **41**, 1293 (1990).
[21]A. Wolf, L. Hutten, and H. Poth, CERN Report No. CERN-EP 84-01 (1984).
[22]H. Danared (private communication).
[23]V. I. Kudelainen, V. A. Lebedev, I. N. Meshkov, V. V. Parkhomochuk, and B. N. Sukhina, Zh. Eksp. Teor. Fiz. **83**, 2056 (1982) [Sov. Phys.—JETP **56**, 1191 (1982)].
[24]F. Brouillard and W. Claeys, in *Physics of Ion-Ion and Electron-Ion Collisions*, edited by F. Brouillard and J. W. McGowan (Plenum, New York, 1983), p. 415.
[25]L. H. Andersen, P. Hvelplund, H. Knudsen, and P. Kvistgaard, Phys. Rev. Lett. **62**, 2656 (1989).